

On cluster embedding schemes based on orbital space partitioning

Ulrich Gutdeutsch, Uwe Birkenheuer, Sven Krüger, and Notker Rösch^{a)}
Lehrstuhl für Theoretische Chemie, Technische Universität München, D-85747 Garching, Germany

(Received 4 November 1996; accepted 3 January 1997)

The embedding approach to the electronic structure of local perturbations in extended systems is based on the fundamental assumption that beyond a certain region around the defect, the properties of the environment are not altered by the presence of the defect. In many computational schemes the resulting subdivision of the defect system into a central and an external region is defined in terms of orbital basis functions. The fundamental embedding assumption then translates into a partitioning of matrix representations, accompanied by fixing the external region contributions to their values in the unperturbed reference system. With the help of density functional cluster-in-cluster embedding calculations we have investigated the quality of this assumption without introducing any additional approximation as usually done to arrive at a computationally feasible embedding scheme. The fundamental embedding assumption is found to cause spurious virtual orbital admixtures to the density matrix which lead to artifacts in the results of embedding calculations. To minimize these undesirable effects, a special "class orthogonalization" scheme has been employed. It allows a perfect reproduction of the defect induced charge density changes as judged by cluster-in-cluster model calculations for a hydrogen substitutional defect in large Li_n clusters (with n up to 309). However, equilibrium geometries, total energies, and vibrational frequencies calculated with this embedding scheme do not exhibit any improvement over results from calculations employing the corresponding nonembedded model clusters. The reason for this failure which prevents the expected convergence of the calculated results with increasing cluster size is analyzed. Thus, from a pragmatic point of view, "naked" cluster models are preferable, at least for metal substrates, due to their relative computational simplicity. Possible techniques to either avoid the virtual orbital admixtures or to improve the quality of the total energies obtained from the embedding calculations are discussed together with the drawbacks of these schemes. © 1997 American Institute of Physics. [S0021-9606(97)00514-X]

I. INTRODUCTION

Ever since first principles quantum mechanical calculations have been established as a powerful tool for studying the microscopic structure of solids and molecules, embedding schemes have been developed to extend the applicability of these new methods toward more complex systems. So far, a bewildering variety of different embedding schemes have been suggested.¹⁻⁴⁹ They all share the concept of partitioning the system under investigation into a central region which contains the structure of interest (a defect, a functional group, an adsorbate complex, etc.) and a surrounding external region. The impact of this "environmental" region on the central region is considered as non-negligible, yet of less importance so that it may be represented only approximately to reduce the effort of the calculations or to even make the calculations feasible at all. Of course, the central region is described at as high a level of sophistication as deemed necessary for properly representing the physical situation at hand. This fundamental partitioning into an embedded cluster and an "indented" environment is often visualized as a direct subdivision in real space, as actually implemented by Greens function matching techniques.¹⁻⁶ Alternatively, it may simply be given by the different levels of theory at which the two regions are treated, as in cases where a cluster

is embedded in an array of point charges,^{7,8} in a crystal field,^{9,10} in a homogeneous dielectric medium,¹¹⁻¹³ or in a shell model representation of the environment.¹⁴⁻¹⁶ More generally, the partitioning of the system is implemented as a division of the variational Hilbert space into appropriate functional subspaces.¹⁷⁻⁴⁶ These subspaces are most commonly defined by means of localized basis functions which are introduced to span (not completely, but sufficiently accurately) the Hilbert space of either the central region only, or of the entire system of interest. Among these techniques one may further distinguish between methods with a dynamic partitioning, such as the group function schemes based on localized orbitals³⁰⁻³² or the concept of Whitten,³³⁻³⁵ which takes into account the actual electronic structure at the region interface when constructing the two regions, and partitioning schemes which are based on a fixed choice of the functional subspaces, like in the various embedding techniques proposed by Pisani.³⁶⁻⁴¹

To arrive at an embedding scheme of practical use, approximations concerning the electronic structure of the external region and its influence on the embedded cluster have to be introduced. As long as there is a distinct chemical separation between the part considered as central region and its surrounding, as is obvious for molecules in solvents or for weakly bound adsorbates, a simple cluster-in-environment approach often is appropriate. Thereby, the embedded cluster is treated as an almost isolated particle, except that contribu-

^{a)} Author to whom all correspondence should be addressed.

tions of the external region to the Hamiltonian are represented by some approximative terms which are not necessarily simpler, but are at least easy enough to obtain. A similar approach may be applied to systems with strong ionic interactions between the two regions, as long as no significant covalent bonding and charge rearrangement occurs across the region boundary.⁷⁻¹⁶ However, for less ionic, covalent, or even metallic environments with direct contact to the central region, like in defect and chemisorption systems, or when functional groups within larger molecules are taken to make up the environment, proper boundary conditions for the wave function of the embedded cluster have to be taken into account.^{1-6,17-49} Such a physical situation requires a partitioning of the wave functions or, alternatively, of the density matrix of the system. In these cases, one of the most commonly adopted assumptions, the so-called “fundamental embedding assumption,” is to take the density matrix, or even its energy resolved contributions (the projected density of states), in the external region to be essentially independent of the specific structure and composition of the inner part of the central region. This allows one to evaluate the contribution to the Hamiltonian and to the total energy of the embedded cluster due to the “indented” environment once and forever in a separate and, in general, much easier calculation.

The moderately large embedded cluster (MLEC) technique, which was originally designed as a Hartree–Fock embedding scheme,^{36,37} and which we have adapted to set up a density functional embedding scheme (DF-MLEC) intended for applications to infinite metallic substrates,^{45,46} is one of these methods which rest on this fundamental embedding assumption. The EMBED program based on the perturbed cluster equations is another one.³⁹⁻⁴¹ The assumption of an essentially unperturbed external region density matrix is not beyond criticism, despite the successful application of both of these methods to a variety of defect and adsorbate systems with various substrates and host crystals.^{44-46,50-52} Experience shows that the approximations unavoidably introduced by the fundamental embedding assumption may affect binding and defect formation energies up to the order of a few tenths of an eV for some critical combinations of adsorbate, substrate, and basis sets employed, and thus may significantly exceed what is commonly accepted as “chemical accuracy.” If these observations pointed to a specific methodological problem, embedded cluster calculations would not perform better on energetics than common nonembedded model cluster calculations.⁵³ Such a conclusion would seriously question the motivation for using the more complicated and often also significantly more demanding embedding approach, at least for situations where accurate total energies are important.

It is the goal of the present work to assess this “fundamental embedding assumption,” which is crucial for the applicability of many schemes. To this end, we will isolate the effects which occur when the density matrix in the external region of a complex system is replaced by a reference density matrix from the effects of additional approximations that are generally invoked to arrive at a computationally efficient embedding scheme. To have access to the exact electronic

structure of the defect system, and to be able to restrict the approximation exclusively to introducing the reference density matrix, we have adopted a cluster-in-cluster embedding approach in the present investigation. Although embedding schemes are generally designed to yield reasonable results already for relatively small central clusters, it is important to check cluster convergence. This may perhaps not be necessary in routine applications, but has to be done in benchmark studies like the present one in order to evaluate the reliability of a method. With this in mind, two rather simple, yet quite realistic test systems have been chosen for the present study: a vacancy and a hydrogen substitutional defect in icosahedral lithium clusters. By this choice, rather large host systems may be treated with a density functional method.

Before turning to the actual cluster-in-cluster test calculations, various ways of establishing a partitioning in functional space will be discussed. Subsequently, the results on the validation of the embedding assumption are presented in two steps. First, the necessity of a balanced orthogonalization scheme for the orbital space partitioning is demonstrated, and then the influence of the approximated density matrix on the charge distribution and on the formation energies of the defects is discussed.

II. THE CONCEPT OF ORBITAL SPACE PARTITIONING

In embedding schemes which employ localized, and preferentially atom-centered orbital basis functions to represent the electronic one-particle wave functions the partitioning of the density operator \hat{P} is usually established by blocking its matrix representation P according to

$$P = \begin{pmatrix} P_{CC} & P_{CD} \\ P_{DC} & P_{DD} \end{pmatrix}. \quad (1)$$

Here, C denotes the part of the matrix indices attributed to the embedded cluster which, in general, consists of an adsorbate or defect region A and a surrounding interface region B ; D denotes the part assigned to the indented environment. The fundamental embedding assumption then reads

$$P = \begin{pmatrix} P_{CC} & P_{CD}^f \\ P_{DC}^f & P_{DD}^f \end{pmatrix} \quad \text{or} \quad P = \begin{pmatrix} P_{CC} & P_{CD} \\ P_{DC} & P_{DD}^f \end{pmatrix} \quad (2)$$

depending on whether only the “cluster–cluster” subblock P_{CC} is allowed to relax with respect to the reference density matrix P^f (as is the case in the MLEC formalism^{36-38,45,46}) or whether the overlap contributions P_{CD} and P_{DC} are allowed to relax as well (like in the EMBED methodology³⁹⁻⁴¹). We envisage a *modified* self-consistent field (SCF) procedure, Kohn–Sham or Hartree–Fock, where approximation (2) is applied in each cycle, though one might also conceive a strictly variational formalism based on this fundamental embedding assumption (see Sec. VI for further discussion). For two reasons the matrix blocking strategy of Eq. (2) does not lead to a *unique* partitioning of the density operator. First, the density matrix may either be taken as a twofold contravariant representation

$$P = (P^{ij})_{i,j=1,\dots,N} \quad \text{with} \quad \hat{P} = \sum_{ij} |\varphi_i\rangle P^{ij} \langle \varphi_j|, \quad (3)$$

as is common in quantum chemistry, but it may also be regarded as a twofold covariant representation

$$P = (P_{ij})_{i,j=1,\dots,N} \quad \text{with} \quad P_{ij} = \langle \varphi_i | \hat{P} | \varphi_j \rangle, \quad (4)$$

or as any of the possible mixed representations with co and contravariant indices. Unfortunately, in the quantum chemistry literature the type of matrix representations actually employed is often not clearly indicated and the tensor notation of Eqs. (3) and (4), ideally suited for this purpose, is hardly used. Second, the matrix representation P is only defined up to unitary transformations which may be applied to the complete basis set $C \cup D$ without actually changing the variational space of the total system. As soon as basis functions assigned to region C and region D are mixed by such a unitary transformation, different partitioning schemes are described by Eq. (1). In principle, any of these partitioning schemes might be adopted, and the question on the most suitable scheme is still subject of discussion. There are, however, certain restrictions, in case an orbital space partitioning is not only applied to the density operator (or to the Greens operator to which the former one is closely related), but also to quantities like the Hamilton or Fock operator. Because in practical implementations relations such as

$$(z - \hat{H}) \hat{G}(z) = \hat{1} \quad \text{or} \quad \langle \hat{A} \rangle = \text{tr}(\hat{P} \hat{A}) \quad (5)$$

are interpreted as matrix equations, the representations adopted for the various operators are associated with each other, unless the matrix equations are extended appropriately by metric tensors g_{ij} and g^{ij} (which are given by the overlap matrix $g_{ij} = \langle \varphi_i | \varphi_j \rangle$ and its inverse, respectively). Here, we refrain from giving any details (for explicit expressions see, e.g., Ref. 54), but will focus on the partitioning of the density matrix as the central quantity to which the fundamental embedding assumption is applied.

In the course of optimizing the DF-MLEC formalism^{45,46} we have tested various partitioning schemes for the density matrix, among them the common twofold contravariant partitioning in the original atom-centered basis set. The use of the standard contravariant density matrix results in problems with the conservation of charge on that part of the system which is to be treated self-consistently. As evident from

$$N = \text{tr}(SP) = \text{tr}(S_{CC}P_{CC}) + \{2 \text{tr}(S_{CD}P_{DC}^f) + \text{tr}(S_{DD}P_{DD}^f)\} \quad (6)$$

the number of electrons attributed to the ‘‘relaxed’’ part of the density matrix,

$$N_C = \text{tr}(S_{CC}P_{CC}), \quad (7)$$

differs from the sum of the nuclear charges Z_C of the embedded cluster due to the overlap population $2 \text{tr}(S_{CD}P_{DC}^f)$. For a metallic Li substrate an electron charge defect of up to 10% was encountered⁴⁵ even for unperturbed substrate clusters; conversely, the twofold covariant partitioning leads to electron numbers N_C much larger than the sum of nuclear

charges of the embedded cluster. These nonvanishing purely formal net charges of the unperturbed embedded substrate clusters do not cause any problems during the evaluation of the CC subblock of the Hamiltonian of the embedded system as long as the ‘‘crystal field’’ correction ΔH is evaluated exactly as in the Hartree–Fock based EMBED program.⁴⁰ This crystal field correction is defined as

$$\Delta H = H_{CC}[P] - H_{\text{isolated}}[P_{CC}], \quad (8)$$

with H_{isolated} being the Hamiltonian of the embedded cluster treated as an isolated species. It totally compensates those contributions to the Hartree potential of the isolated cluster Hamiltonian H_{isolated} which result from the arbitrary decomposition of the electron overlap population entering N_C . However, the crystal field correction is not easy to calculate as all non-negligible matrix elements between the central region and the, in principle, infinite external region have to be computed. A further complication in case of a density functional implementation is caused by the nonlinearity of the exchange-correlation functional with respect to the density. On the other hand, with the crystal field correction ΔH treated approximately as

$$\Delta H \approx \Delta H^f = H_{CC}^f[P^f] - H_{\text{isolated}}[P_{CC}^f], \quad (9)$$

where ΔH^f is the crystal field correction from a reference calculation on a defect free system, it turned out to be rather difficult to compensate the Coulomb potential of the artificial charge contributions to $Z_C - N_C$ to sufficient accuracy, especially in the vicinity of some adsorbates which was the kind of defect we were primarily interested in when developing the DF-MLEC scheme.^{45,46} This situation arises because the variational space of the reference system only partially covers the variational space of the adsorbate, and hence a kind of truncation in the approximated crystal field correction ΔH^f occurs near the adsorbate. In response to this problem, we have developed⁵⁵ an extrapolation scheme based on arrays of atom-centered point charges around the embedded cluster. The point charges are optimized in such a way that the matrix elements of ΔH^f on substrate atoms in the direct vicinity of the adsorbate are reproduced, as well as possible, by the corresponding matrix elements of the electrostatic potential of the point charges. To arrive at a well-defined and numerically stable fitting procedure, and also to guarantee a sensible extrapolation of the resulting electrostatic potential into the region of the adsorbate, the variational freedom of the point charges is reduced by constraints which only allow the major multipole contributions around the adsorbate to be corrected. This technique has successfully been employed to extrapolate the missing Coulomb contribution to ΔH^f into the adsorbate’s variational space.⁵⁵

Yet other problems remain, the most important of them is related to the fact that the elements of the MLEC matrices coupling the central region to the outer region (for their definition see Ref. 37) were found to become rather large when a twofold covariant density matrix partitioning scheme was employed; this entails serious numerical instabilities. Similar problems were encountered for twofold contravariant partitioning within the MLEC embedding scheme⁴⁵ in line with

previous findings of other research groups.^{36,37,42,43} These difficulties are independent of how the cluster Hamiltonian $H_{CC}[P]$ is actually set up, and most likely they also occur in the EMBED formalism since the EMBED coupling matrices are closely related to the MLEC matrices.³⁹

One way to avoid spurious charge contributions on embedded clusters as well as undesirable numerical instabilities is to partition the density matrix in an *orthonormal* basis set of the entire variational space $C \cup D$.^{42–46} Then the distinction between co and contravariant representation becomes superfluous, but it is crucial choosing the orthogonalization in a balanced way. To illustrate this point consider an orthonormal basis set which is generated by simply orthogonalizing the basis functions of the external region onto those of the central region before any intraregion orthonormalization is carried out. This partitioning scheme would be equivalent to a twofold covariant partitioning as far as the cluster–cluster subblock of the density matrix is concerned, and thus the difficulties discussed above remain. Similarly, pre-orthogonalization of the central region basis functions onto the basis functions of the external region with subsequent intraregion orthogonalization leads to an embedding scheme which is equivalent to that where the twofold contravariant form of the density matrix is partitioned directly. Symmetric orthogonalization appears to be the ideal procedure for generating an appropriate orthonormal basis set. This strategy will be employed for parts of the calculations of the present investigation. However, as will be discussed in Sec. IV, an even more balanced orthogonalization scheme had to be developed to finally arrive at an acceptable partitioning.

III. METHOD AND MODEL SYSTEMS

Two types of model defect systems will be studied in the present work: a lithium vacancy as well as a substitutional hydrogen impurity in metal-like lithium. The metallic host system is simulated by clusters of up to 309 Li atoms. For computational efficiency, these model systems are chosen to exhibit icosahedral symmetry, comprising up to four icosahedral shells. The intershell distance of the Li icosahedra is fixed at the experimental nearest-neighbor lithium distance of bcc bulk lithium, 3.022 Å,⁵⁶ resulting in a slightly expanded intrashell lithium distance of 3.178 Å. To create the defect the central Li atom is either removed or substituted by a hydrogen atom. The surrounding nearest-neighbor shell of 12 Li atoms is geometrically relaxed unless stated differently. The geometry of all further shells is chosen to coincide with that of the unperturbed reference host system. Only the outermost shell will be regarded as the external region because size convergence of the embedded cluster is more important in the present context than convergence of the indented environment toward a realistic infinite bulklike “host crystal.” The defect systems constructed in this way will be denoted by either $X\text{Li}_n(12+m+k^f)$ or $X\text{Li}_n(12^*+m+k^f)$ depending on whether a geometrical relaxation of the first icosahedral shell is taken into account (12^*) or models with an unchanged geometry of the nearest-neighbor shell around the defect are being considered (12). m and k denote the

numbers of those lithium atoms in the remaining icosahedral shells which belong to the embedded cluster C and to the environment D , respectively. X designates the atom at the center of the icosahedron (if any), and the upper index “ f ” indicates the use of a reference density P^f in the external region. For exact cluster calculations the corresponding notations are $X\text{Li}_n(12+m)$ and $X\text{Li}_n(12^*+m)$, where m is the total number of Li atoms beyond the first icosahedral shell.

The cluster calculations as well as the cluster-in-cluster embedding calculations were carried out with a suitably modified version of the LCGTO-DF (linear combination of Gaussian-type orbitals-density functional) code.⁵⁷ The orbital basis sets, $(9,4) \rightarrow [4,2]$ for Li and $(6,1) \rightarrow [3,1]$ for H, as well as the basis sets for representing the electron charge density and the exchange-correlation potential, $(9s,2d_{r,2},5p)$ for Li and $(6s)$ for H, are taken from previous cluster-in-surface embedding studies.^{45,46} The local density approximation to the exchange-correlation functional as parametrized by Vosko *et al.*⁵⁸ is used throughout this study.

In all embedding calculations presented in the following, the orbital space partitioning according to Eq. (2) is realized by means of an orthonormal basis set which is generated via an intermediate orthonormalization step. To this end, the standard SCF procedure is modified as follows. Once the Kohn–Sham orbitals of the complete defect system and the corresponding one-particle energies have been obtained, a trial Fermi level is chosen, and (a) fractional occupation numbers are determined by Gaussian broadening (0.3 eV) of the cluster level spectrum.⁵⁹ Then, (b) the cluster density matrix is set up as usual and transformed into the representation of the intermediate orthonormal basis set. Next, (c) the external region subblocks of the density matrix are replaced by those of the reference density matrix which has been obtained before in a separate calculation of the corresponding unperturbed lithium cluster. Finally, (d) the total number of electrons is computed from the new density matrix, and a new step (a) is carried out after a suitable adjustment of the Fermi level. This procedure is iterated until the formal, pre-assigned number of electrons of the complete defect system is reached. Except for the constraint imposed by Eq. (2) the charge distribution is allowed to relax freely over the whole defect system, and the total energy is evaluated as in a standard cluster calculation without resorting to any further approximation. Since replacing density matrix subblocks, in general, violates charge conservation, the Fermi energies determined for the exact cluster and for the corresponding cluster-in-cluster embedding calculation will differ. However, for systems where the fundamental embedding assumption is justified, no significant differences are expected. Both strategies of replacing the subblocks of the external region mentioned in Eq. (2), only the DD subblock and all but the CC subblock, will be considered in this study.

The Fermi level adjustment described above closely follows the concepts developed for the DF-MLEC form-

alism.^{45,46} It is based on the idea that for overall neutral defects any charge concentration (or abstraction) at the defect site is completely screened *within* the embedded cluster. Of course, this requires the embedded cluster to be sufficiently (“moderately”) large. Alternatively, one could allow for some charge transfer across the boundary of the embedded cluster even though the external region subblocks of the density matrix are kept fixed.⁶⁰ This is justified because an infinite indented host system may act as a perfect electron reservoir without any changes in its electronic structure. However, to account for the energy connected to this charge exchange, a chemical potential has to be introduced⁶⁰ which is found to be quite distinct from the Fermi level of the host crystal. Furthermore, this chemical potential may significantly depend on the shape and composition of the boundary of the embedded cluster.^{60,61}

IV. OPTIMIZATION OF THE PARTITIONING

Orbital space partitioning, though a quite natural scheme at first glance, conceals an intrinsic problem as far as the wave functions are concerned. Let ψ_n be one of the occupied orbital wave functions of the target system, i.e., the *complete* defect system, which is composed of contributions from regions C and D

$$\psi_n = \psi_n^C + \psi_n^D \quad (10)$$

according to the intermediate orthonormal basis set. Each of the two contributions may be reexpanded in the complete set of eigenfunctions of the defect system,

$$\psi_n^C = \sum_m \psi_m a_{mn}^C, \quad \psi_n^D = \sum_m \psi_m a_{mn}^D. \quad (11)$$

In general, there will be admixtures of all kinds of orbitals, occupied as well as virtual ones, in both parts ψ_n^C and ψ_n^D , but as long as no approximations are introduced these contributions will cancel exactly,

$$a_{mn}^C + a_{mn}^D = \delta_{mn}. \quad (12)$$

However, replacing the external region contribution ψ_n^D by that of an unperturbed reference system leads to

$$\tilde{\psi}_n = \psi_n^C + \psi_n^{D,f} = \sum_m \psi_m (a_{mn}^C + a_{mn}^{D,f}). \quad (13)$$

Since the cancellation according to Eq. (12) will no longer be perfect, admixtures of high-energy virtual states may occur in the approximated occupied orbitals $\tilde{\psi}_n$ which, in turn, significantly distort the electronic structure and the total energy of the approximated defect system. Replacing regional contributions to orbitals is not equivalent to replacing density matrix subblocks, nevertheless it provides some insight into the impact of a procedure where orbital space partitioning is combined with freezing contributions from the external region. Most likely there will be some similar high-energy virtual states admixture in density matrix partitioning schemes as well.

To manifest such admixtures in the approximated density matrix \tilde{P} obtained from a self-consistent embedding calculation, the difference

$$\Delta P = \tilde{P} - P \quad (14)$$

with respect to the corresponding exact density matrix P (resulting from a standard SCF calculation on $C \cup D$) will be analyzed as follows. To first order the difference in total energy between the embedding calculation and the exact calculation is given by

$$\Delta^{(1)}E = \text{tr}(\Delta PH) = \sum_n \langle \psi_n | \Delta P | \psi_n \rangle \epsilon_n = \sum_n \Delta_n \epsilon_n, \quad (15)$$

with ψ_n being the eigenfunctions from the exact reference calculation and ϵ_n the associated eigenvalues. The difference in total electron charge

$$\Delta Q = \text{tr}(\Delta PS) = \sum_n \langle \psi_n | \Delta P | \psi_n \rangle = \sum_n \Delta_n, \quad (16)$$

on the other hand, has to vanish because of the Fermi level adjustment discussed in Sec. III. However, the fact that this sum over the orbital resolved density matrix difference Δ_n vanishes does not guarantee that the energy weighted sum in Eq. (15) does so as well, or even stays small. To visualize the orbital resolved density matrix differences, we introduce sign-sensitive, and locally integrated orbital resolved density matrix differences

$$Q^\pm(\epsilon, \Delta\epsilon) = \sum_n' (\Delta_n \pm |\Delta_n|)/2, \quad (17)$$

where the prime indicates summation over orbital energies ϵ_n subject to $\epsilon - \frac{1}{2}\Delta\epsilon < \epsilon_n \leq \epsilon + \frac{1}{2}\Delta\epsilon$. We also define the related energy contributions $E^+(\epsilon, \Delta\epsilon)$ and $E^-(\epsilon, \Delta\epsilon)$ to the first-order energy difference $\Delta^{(1)}E$, e.g.,

$$E^+(\epsilon, \Delta\epsilon) = \sum_{\Delta_n > 0}' \Delta_n (\epsilon_n - \epsilon_F). \quad (18)$$

The quantities defined in Eqs. (17) and (18) are similar in spirit to density of states, and may easily be displayed as histograms. The reason for introducing the sign sensitivity is to document the random scattering signs of the individual contributions Δ_n which otherwise would cancel to a large extent during the local integration. For convenience, the Fermi level ϵ_F has been chosen as zero energy in Eq. (18).

Figure 1 shows the quantities $Q^\pm(\epsilon, \Delta\epsilon)$ and $E^\pm(\epsilon, \Delta\epsilon)$ for the defect system $\text{HLi}_{146}(12+42+92^f)$. The orbital partitioning in this example is based on a symmetrically orthogonalized basis set, and all but the CC subblocks of the density matrix have been replaced here. As expected, the main contributions are gathered around the Fermi level (at -3.0 eV), but obviously, there also are significant high-energy virtual orbital admixtures with energies up to almost 200 eV. Even some admixtures of Li $1s$ core orbitals (between -48.8 and -49.9 eV) are discernible (see the inset) and it is evident from Fig. 1(b) that there is little hope for the energy weighted orbital resolved density matrix differences $\Delta_n(\epsilon_n - \epsilon_F)$ to sum up to zero. Actually $\Delta^{(1)}E = 1.35$ eV in

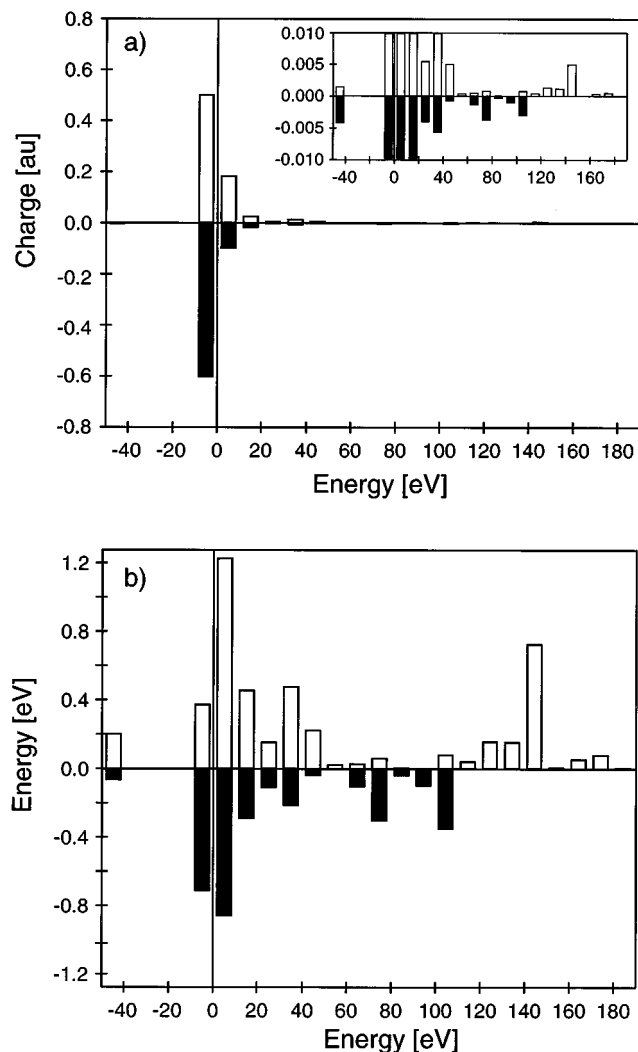


FIG. 1. Plain (a) and energy weighted (b) orbital resolved density matrix differences $\Delta_n = \langle \psi_n | \Delta P | \psi_n \rangle$ of the $\text{HLi}_{146}(12+42+92^f)$ defect system due to the fundamental embedding assumption. The orbital space partitioning scheme considered here is the one based on a symmetrically orthogonalized basis set with all but the CC subblocks of the density matrix being replaced (see the text for details). Shown are the sign-sensitive and locally integrated quantities $Q^\pm(\epsilon, \Delta\epsilon)$ and $E^\pm(\epsilon, \Delta\epsilon)$ as defined in Eqs. (17) and (18) with $\Delta\epsilon = 10$ eV. The insert focuses on contributions with small absolute values.

this example. During symmetric orthogonalization localized basis functions acquire admixtures from diffuse basis functions of neighboring atoms, and vice versa, and thus a strong interlocking of the two functional subspaces C and D takes place. As a consequence the region contribution coefficients a_{mn}^C and a_{mn}^D of each occupied orbital become much larger than one would expect from the neglect of the defect induced changes in the electronic structure of the external region. Even core orbitals in the central region, if located near the region boundary, require admixtures of orthonormal basis functions from the *external* region, in order to compensate all of the diffuse atom-centered basis functions which have been added to the core orbital-like atomic basis functions in the course of the symmetric orthogonalization. In systems with heavier elements this holds for both core as well as ‘‘semicore’’ states. All these admixtures are artificial and

only introduced by the intermediate basis set.

The results displayed in Fig. 1 leave little hope for a successful formalism that implements the fundamental embedding assumption in a straightforward fashion. To arrive at a physically more meaningful orthogonalization, the original atom-centered basis functions are divided into various classes of ‘‘chemically separated’’ orbitals, such as core orbitals, valence orbitals, and polarization functions, and Schmidt orthogonalization (in order of increasing energy) is applied for the interclass preorthogonalization, while a symmetric orthonormalization is used for the intraclass orthogonalization. This scheme, which in the following shall be denoted as ‘‘class orthogonalization,’’ takes advantage of the geometrical balance of the symmetric orthogonalization between orbitals of the same kind, and at the same time prevents that localized atom-centered basis functions for the core (and valence) orbitals to become contaminated by polarization functions and basis functions for atomic orbitals of higher energy. A similar strategy has successfully been applied previously⁶² to avoid unbalanced core orbital admixtures to configuration–interaction spaces which are especially set up to study localized chemical bonds in extended systems. The positive effect of the class orthogonalization can be seen in Fig. 2 which shows data for the same system as in Fig. 1, yet is computed by means of a class orthogonalization. Three classes of basis functions have been introduced for the Li atoms: the $1s$ core orbitals of all atoms, the $2s$ and $2p$ valence orbitals (orthogonalized on the core class), and the $3s$, $3p$, and $4s$ polarization functions (orthogonalized on the core and the valence classes). As expected, the Li $1s$ core orbital contamination of the density matrix difference vanishes completely (see the insert of Figs. 1 and 2), and the overall amount of high-energy virtual orbital admixtures is significantly reduced (cf. Figs. 1 and 2). Furthermore, the energy weighted orbital resolved density matrix differences $E^\pm(\epsilon, \Delta\epsilon)$ now tend to zero with increasing one-particle energies, which was not the case for the embedding calculation based on orbitals that had been simply subjected to symmetric orthogonalization. In addition, the first-order energy difference $\Delta^{(1)}E$, -0.50 eV, is significantly reduced in magnitude compared to the previous results. Clearly, class orthogonalization achieves a much more balanced orbital space partitioning of the density matrix than symmetric orthogonalization. Common contravariant partitioning, on the other hand, turned out to be much worse with $\Delta^{(1)}E = -15.9$ eV for $\text{HLi}_{146}(12+42+92^f)$.

V. EVALUATION OF THE EMBEDDING SCHEME

Orbital space partitioning based on class orthogonalization, as has been shown in Sec. IV, substantially reduces the negative impact of the fundamental embedding assumption as compared to other orthogonalization/partitioning schemes. Yet, it remains to be verified whether the approximation involved provides a reasonable description of the electronic structure of an embedded cluster. This will be done in two steps: first, we will examine in detail the charge distribution of the defect system $\text{HLi}_{146}(12+42+92^f)$, and then we will

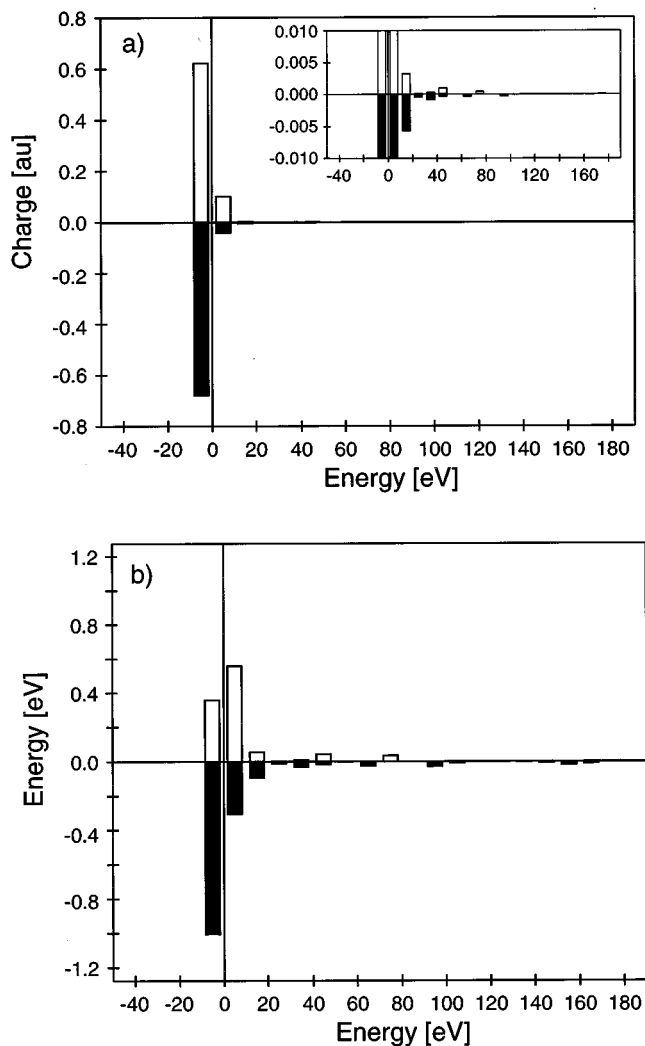


FIG. 2. Plain (a) and energy weighted (b) orbital resolved density matrix differences $\Delta_n = \langle \psi_n | \Delta P | \psi_n \rangle$ of the $\text{HLi}_{146}(12+42+92^f)$ defect system due to the fundamental embedding assumption as in Fig. 1, but with an orbital space partitioning based on a class orthogonalized basis set.

compare typical defect formation characteristics in a series of embedded cluster models comprising up to 308 Li atoms.

Figure 3(a) shows the difference between the self-consistent density of an embedded cluster calculation for $\text{HLi}_{146}(12+42+92^f)$, with only the external region subblock P_{DD} being replaced [the second variant of Eq. (2)] and that of a normal SCF calculation of the whole defect system $\text{HLi}_{146}(12+134)$. The overall charge density difference is remarkably small (less than 10^{-4} a.u.). It is completely restricted to the external region which is the outer shell of the LiLi_{146} icosahedron in the present case. The charge distribution in the central region is almost perfectly reproduced by the embedding calculation (the lowest value of the contour lines: $\pm 3.2 \times 10^{-5}$ a.u.). If the subblocks P_{CD} and P_{DC} are replaced as well [the first variant in Eq. (2)], the fundamental embedding assumption is expected to be fulfilled to a lower degree. This is indeed the case [Fig. 3(b)], yet the charge density differences remain essentially localized near the interface region between the second and the third icosahedral

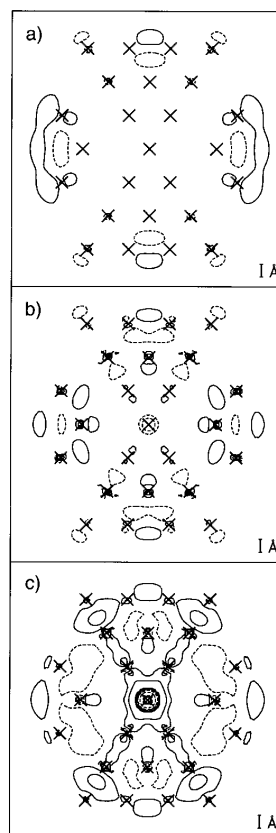


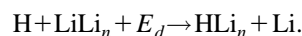
FIG. 3. Charge density difference maps of the defect system $\text{HLi}_{146}(12+134)$ displayed in one of the fifteen equivalent mirror planes of the icosahedral cluster. Shown is the quantity $\rho(\text{HLi}_{146}(12+42+92^f)) - \rho(\text{HLi}_{146}(12+134))$ for cases where (a) only the subblock P_{DD} of the density matrix has been replaced or (b) all subblocks except P_{CC} . Panel (c) displays the corresponding difference map $[\rho(\text{HLi}_{54}(12+42)) - \rho(\text{HLi}_{146}(12+134))] - [\rho(\text{LiLi}_{54}) - \rho(\text{LiLi}_{146})]$ for a non-embedded cluster calculation. The values of the contour lines are $\pm 0.000\ 032$, $\pm 0.000\ 10$, $\pm 0.000\ 32$, ± 0.0010 , ± 0.0032 , and ± 0.010 a.u. with positive and negative differences represented as solid and dashed lines, respectively. The positions of the atoms in the displayed plane are marked (\times).

shells. Some minor impact on the defect center is also discernible. Obviously, the transfer of electron charge density onto the more electronegative hydrogen atom is already suppressed to some extent when the overlap subblocks P_{CD} and P_{DC} of the density matrix are fixed to their values in the unperturbed reference host system. Still, the differences in the charge density are small compared to those typically obtained by nonembedded model cluster calculations, e.g., for the $\text{HLi}_{54}(12+42)$ model of the HLi_{146} defect system shown in Fig. 3(c). Here, a profound difference is discernible between the induced charge rearrangement around the substitutional hydrogen as predicted by the nonembedded cluster model and that of the complete defect system (more than 3.2×10^{-4} a.u. in the immediate vicinity of the hydrogen atom). In summary, proper cluster embedding certainly leads to a substantially improved description of a defect system as far as the charge distribution is concerned, and consequently of all related quantities like the dipole moment and atomic charges.

TABLE I. Comparison of the defect formation energies of a Li vacancy and a hydrogen substitutional defect in Li icosahedra obtained by various embedded and nonembedded model calculations. The reference energies E_d in the second column result from full SCF calculations on the complete defect systems. The columns headed by P_{DD}^f and $P_{CD}^f, P_{DC}^f, P_{DD}^f$ refer to the two variants of replacing the density matrix sub-blocks [see Eq. (2)]. The nonembedded model clusters are constructed by removing the atoms in the external region (denoted by k^f). Energies are given in eV.

System	E_d	$E_d(\text{model}) - E_d$		
		P_{DD}^f	$P_{CD}^f, P_{DC}^f, P_{DD}^f$	Nonemb.
HLi ₁₂ (12)	0.90			
HLi ₅₄ (12+42 ^f)	1.07	-11.51	+1.66	-0.17
HLi ₁₄₆ (12+42+92 ^f)	0.53	+0.89	-0.50	+0.54
HLi ₃₀₈ (12+134+162 ^f)	0.33	+0.51	-0.15	+0.20
Li ₁₂ (12)	2.67			
Li ₅₄ (12+42 ^f)	2.87	-9.96	+1.75	-0.20
Li ₁₄₆ (12+42+92 ^f)	2.57	+0.55	-0.24	+0.30
Li ₃₀₈ (12+134+162 ^f)	2.51	+0.22	-0.02	+0.06

Next we turn to a discussion of the energetics. Table I summarizes the defect formation energies E_d for a lithium vacancy and for a hydrogen substitutional defect in Li icosahedra. These quantities are defined according to the formal reactions



The defect formation energy of the reference defect system is given in the second column of Table I while the *deviations* due to the two variants of fixing the external region sub-blocks of the density matrix are shown in the next two columns. For comparison, the deviations found for nonembedded model clusters without an external region are also given (the fifth column). No geometrical relaxation of the nearest-neighbor Li shell around the defect has been considered here. Two general trends are discernible. The defect formation energy differences become smaller with increasing cluster size, and the results for the less restrictive embedding scheme (only P_{DD} fixed) are always worse (and opposite in sign) than those of the more restrictive embedding scheme (all but P_{CC} fixed). The former trend was to be expected since the fundamental embedding assumption is satisfied better, the larger the distance between the defect and the cluster boundary. On the other hand, the latter trend is rather surprising, and a much more detailed analysis of individual contributions to the total energy would be required to trace its origin beyond doubt. However, the most important observation in the present context is that the quality of the predicted defect formation energies is generally not improved upon embedding. Only in some cases the defect formation energy from an embedding calculation (with all subblocks of P but P_{CC} fixed) is closer to the target quantity than the corresponding value of the nonembedded cluster calculation, but the energy differences are small (≤ 0.05 eV). Furthermore, the results of

TABLE II. Comparison of various defect formation characteristics of a hydrogen substitutional defect in Li icosahedra obtained from calculations using embedded (class orthogonalization and all but P_{CC} replaced) and nonembedded model clusters. The reference values resulting from full SCF calculations on the corresponding complete defect systems are given in the second column. The quantities considered are: the optimized radius of the nearest-neighbor Li₁₂ shell r_e , the corresponding defect formation energy E_d , and the vibrational frequency ω_e of the totally symmetric shell breathing mode.

System	Reference value	Model induced difference	
		$P_{CD}^f, P_{DC}^f, P_{DD}^f$	Nonemb.
Optimized defect energy E_d (eV)			
HLi ₁₂ (12*)	0.43		
HLi ₅₄ (12*+42 ^f)	1.04	+1.19	-0.61
HLi ₁₄₆ (12*+42+92 ^f)	0.37	-0.36	+0.67
HLi ₃₀₈ (12*+134+162 ^f)	0.13	-0.28	+0.24
Equilibrium shell radius r_e (Å) ^a			
HLi ₁₂ (12*)	2.78		
HLi ₅₄ (12*+42 ^f)	2.97	-0.15	-0.19
HLi ₁₄₆ (12*+42+92 ^f)	2.90	+0.16	+0.07
HLi ₃₀₈ (12*+134+162 ^f)	2.89	-0.14	+0.02
Vibrational frequency ω_e (cm ⁻¹)			
HLi ₁₂ (12*)	251		
HLi ₅₄ (12*+42 ^f)	263	+207	-12
HLi ₁₄₆ (12*+42+92 ^f)	274	+7	-11
HLi ₃₀₈ (12*+134+162 ^f)	268	+11	+6

^aUnrelaxed shell radius: 3.022 Å.

Table I show that embedded clusters with just one neighboring shell around the defect treated self-consistently do not provide appropriate models.

So far only total energies of geometrically unrelaxed defect systems have been discussed, and the question arises whether calculated equilibrium properties show a similar behavior. For this purpose, we decided to study models where the nearest-neighbor shell around the hydrogen substitutional defect is allowed to relax. We have considered only the DF-MLEC-like embedding scheme [the second variant of Eq. (2)]. The computed optimized shell radius, the equilibrium defect formation energy, and the vibrational frequency of the Li₁₂ shell breathing mode of all four HLi_n clusters investigated are summarized in Table II. No significant improvement, if any, is discernible upon embedding for any of these quantities. From these results we are lead to the conclusion that the approximations introduced by the fundamental embedding assumption, though minimized by performing the orbital space partitioning in a class orthogonalized intermediate basis set, are still too strong to yield improved results for the energetics and related quantities than those obtained from the usual nonembedded cluster models.

VI. DISCUSSION

At this point it is instructive to recall that the reliability of the defect formation energies computed with the EMBED program have improved substantially after a variational charge balance correction has been introduced.⁶⁰ This energy correction takes into account the defect induced charge transfer between the embedded cluster and the indented host crys-

TABLE III. Correlation between the deviations ΔE_d of the defect formation energy and of the Fermi level $\Delta \epsilon_F$ due to the fundamental embedding assumption for Li vacancies and hydrogen substitutional defects in Li icosahedra. P_{DD}^f , and $P_{CD}^f, P_{DC}^f, P_{DD}^f$ refer to the first and second variant of the approximations to the density matrix P [see Eq. (2)]. Energies are given in eV.

System	P_{DD}^f			$P_{CD}^f, P_{DC}^f, P_{DD}^f$		
	ΔE_d	$\Delta \epsilon_F$	$\Delta E_d / \Delta \epsilon_F$	ΔE_d	$\Delta \epsilon_F$	$\Delta E_d / \Delta \epsilon_F$
HLi ₁₄₆ (12+42+92 ^f)	0.89	-0.042	-21.1	-0.50	0.016	-31.7
Li ₁₄₆ (12+42+92 ^f)	0.55	-0.026	-21.2	-0.24	0.006	-36.8
HLi ₃₀₈ (12+134+162 ^f)	0.51	-0.024	-21.0	-0.15	0.003	-57.4
Li ₃₀₈ (12+134+162 ^f)	0.22	-0.011	-19.4	-0.02	0.001	-34.7

tal even though the density matrix in the external region is assumed to remain unchanged. Empirically a remarkably linear correlation between the ‘‘missing’’ charge ΔQ and the corresponding change ΔE^q in total energy was found and a correction in the spirit of a chemical potential, $\Delta E^Q = \mu \Delta Q$, has been suggested.^{60,61} A similar correlation is also noticeable in our data (see Table III). Recall the procedure described in Sec. III to ensure a constant electronic charge on the embedded cluster which leads to a change $\Delta \epsilon_F$ of the Fermi level. Using the density of states $\rho(\epsilon_F)$ at the Fermi level, this change may directly be related to the missing cluster charge that would be found if the Fermi level would have been kept fixed, $\Delta Q = \rho(\epsilon_F) \Delta \epsilon_F$. Furthermore, for adjustments $\Delta \epsilon_F$ on the order of a few hundredth of an eV as encountered in the present study (Table III) the linear relation $\Delta E^F = \mu_{\text{clust}} \rho(\epsilon_F) \Delta \epsilon_F$ provides a good estimate of the associated total energy change of the embedded cluster. Thus, together with the missing charge contribution ΔE^Q , the change ΔE_d of the defect formation energy due to the application of the fundamental embedding assumption should read

$$\Delta E_d \approx (\mu_{\text{clust}} - \mu) \rho(\epsilon_F) \Delta \epsilon_F. \quad (20)$$

For the EMBED type of density matrix fixing (P_{DD} only) the correlation between ΔE_d and $\Delta \epsilon_F$ is surprisingly good, the ratio $\Delta E_d / \Delta \epsilon_F$ varies only between -19 and -21. For the DF-MLEC type of fixing the density matrix, the range is much larger (-30 to -60), nevertheless a qualitative correlation exists, too. Therefore some evidence exists that a charge balance correction amends the poor performance of the fundamental embedding assumption for the energetics, and, in turn, improves the geometry and geometry sensitive quantities. However, such a corrective device carries an expost flavor and may be viewed as interfering with the ‘‘first principles’’ character that one generally strives for when designing sophisticated embedding schemes like DF-MLEC or EMBED (see also the remarks on the chemical potential at the end of Sec. III). From a pragmatic point of view it is also worth recalling that embedding schemes are, in general, computationally much more demanding than calculations employing nonembedded model clusters.

According to our understanding, the main reason for the ultimate failure of the orbital space partitioning schemes, at least for metal host systems tested in the present investigation, is related to the mismatch of the functional space par-

tioning used to define the embedded cluster, and that given by the occupied and virtual states of the defect system. This mismatch causes the nonvanishing virtual orbital admixtures

$$\psi_{n,\text{vir}}^C = \sum_m^{\text{vir}} \psi_m a_{mn}^C, \quad \psi_{n,\text{vir}}^D = \sum_m^{\text{vir}} \psi_m a_{mn}^D \quad (21)$$

to the region C and region D contributions of the occupied orbitals discussed in Sec. IV [see Eq. (11) for the notation].

A new method to avoid this mismatch was recently proposed by Head.⁶³ In the light of the present discussion and using the nomenclature introduced here, his idea may be phrased as follows. Let U_C be the functional subspace spanned by the atom-centered basis functions located in the region of the cluster that is to be embedded, and let \hat{P}_{occ} and $\hat{P}_{\text{vir}} = \hat{1} - \hat{P}_{\text{occ}}$ be the projectors onto the occupied and virtual states of the complete, unperturbed reference system (which, for a closed shell system, are directly related to the density operator). Then Head’s formalism corresponds to defining the embedded cluster through its functional subspace,

$$U = U_1 \oplus U_2 \quad \text{with} \quad U_1 = \hat{P}_{\text{occ}}(U_C), \quad U_2 = \hat{P}_{\text{vir}}(U_C), \quad (22)$$

and the indented host crystal through the orthogonal complement $V = U^\perp$. Specifically, the subspace U is constructed⁶³ by orbital rotations which are generated by augmenting the original basis functions of U_C by atomic orbitals from the indented environment in two ways such that the rotated basis functions, on the one hand, exclusively belong to the subspace of the occupied orbitals of the entire reference system (U_1), and on the other hand, exclusively belong to the subspace of the virtual orbitals of the complete unperturbed system (U_2). By construction, U is an extension of the original subspace U_C , which is almost twice as large as U_C . As evident from Eq. (22), U is invariant under \hat{P}_{occ} , which results in a block diagonal matrix representation,

$$P_{\text{occ}} = \begin{pmatrix} P_{UU} & 0 \\ 0 & P_{VV} \end{pmatrix} \quad (23)$$

of the projector \hat{P}_{occ} . Consequently, the occupied orbitals ψ_n of the complete system not only obey $\hat{P}_{\text{occ}} \psi_n = \psi_n$, but also $\hat{P}_{\text{occ}} \psi_n^U = \psi_n^U$ and $\hat{P}_{\text{occ}} \psi_n^V = \psi_n^V$, which immediately leads to

$$\psi_{n,\text{vir}}^U = 0, \quad \psi_{n,\text{vir}}^V = 0. \quad (24)$$

Hence, no virtual orbital admixtures occur in this orbital space partitioning scheme, and there may be a chance to substantially improve the quality of the fundamental embedding assumption. However, there are two aspects to consider. First, it is crucial to recognize that there is no guarantee for the subspace defining the embedded cluster to stay localized in the common sense. Depending on the nature of the host crystal material, the basis functions spanning U_1 and U_2 may become rather extended. Especially for metals one may run into serious problems because of the large number of matrix elements which have eventually to be evaluated and because of the orthogonalization steps necessary to set up the subspace U (for details see Ref. 63). The difficulties encountered⁶³ when this new orbital space partitioning scheme was applied to hydrogen adsorption on-top of a Li(001) monolayer may very well be related to a large (implicit) geometrical extension of the subspace U which is assigned to the embedded Li cluster, and further investigations seem necessary to characterize the type of host systems which may be treated successfully with the method of Head.

The second aspect which has to be taken into account is that the projectors \hat{P}_{occ} and \hat{P}_{vir} depend on the electronic structure of the system considered. Therefore the subspaces U and V , which have been set up for the unperturbed reference system, will in general no longer be perfectly invariant under \hat{P}_{occ} once the defect is introduced. Without specific tests it is hard to judge to which extent this will influence the validity of Eq. (24). If the electronic structure of the defect system is treated within the constrained SCF approach as done in Ref. 63, the block diagonal form of the matrix P_{occ} [Eq. (23)] is guaranteed and no problems arise with Eq. (24). On the other hand, if some coupling between orbitals of the embedded cluster and orbitals of the indented host crystal is allowed *before* the fundamental embedding assumption is applied, there will most likely be high-energy virtual orbital admixture in the density matrix again. To our understanding only a strictly variational approach (like the constrained SCF scheme⁶⁴) is able to yield regional orbital contributions ψ_n^U and ψ_n^V (or ψ_n^C and ψ_n^P) which are fully consistent with the density matrix resulting from the fundamental embedding assumption, and which therefore rules out any spurious virtual orbital admixtures. However, a strictly variational scheme which (in contrast to the constrained SCF approach) also allows orbital coupling between the central region and its environment does not seem easy to design.

VII. SUMMARY AND CONCLUSIONS

In specific implementations of embedding schemes it is generally difficult, if not impossible, to separate numerical and computational approximations from those approximations which arise from the fundamental embedding assumptions of the underlying method. The former type of approximations are introduced to simplify the algorithm or to save computer time; in principle, they can be eliminated as far as necessary. On the other hand, the latter approximations have to be regarded as intrinsic to an embedding formalism. They limit the overall accuracy of an embedding scheme, and thus

it is important to check their quality and consequences. By restricting ourselves to pure cluster-in-cluster embedding we were able to exclusively focus on the fundamental embedding assumption which is generic to embedding schemes that are based on orbital space partitioning [see Eq. (2)] and to avoid any further approximations with regard to the theoretical and computational treatment of the reference defect system. Vacancy and hydrogen substitutional defects in large Li icosahedral clusters have been chosen as test cases.

Matrix blocking and subsequent replacement of the subblocks which refer to the external region [see Eq. (2)] is an algorithmic scheme rather than a definite procedure because its concrete meaning strongly depends on the underlying orbital basis set and on the matrix representation adopted. In order to arrive at an orbital space partitioning scheme which is well suited for embedding, it turned out to be extremely important, especially for total energy calculations on metal host systems, to reduce as much as possible the spurious admixtures of virtual orbitals. These contaminations of the density matrix are unavoidably introduced if one implements the fundamental embedding assumption by means of orbital space partitioning. A special orthogonalization scheme, termed "class orthogonalization," has been employed to minimize these undesirable consequences, and it was found that performing the orbital space partitioning in such a class orthogonalized basis set yields the best results with respect to the spurious virtual orbital admixtures.

Defect induced charge rearrangement (and related quantities) were found to be almost perfectly reproduced by a cluster-in-cluster embedding calculation based on the class orthogonalization partitioning scheme. The fundamental embedding assumption is obviously well-suited for that purpose. However, as far as the energetics and the geometry of the defect systems investigated is concerned, we found that the embedding calculations did not perform any better than straightforward nonembedded cluster model calculations for the defect system. Although minimized by the class orthogonalization, an effect of the virtual orbital admixtures on the total energy, of the order of a few tenths of an electron volt, seems to remain. Thus accuracy is not improved beyond that of nonembedded cluster models of comparable size which are generally computationally far less demanding than the corresponding embedded cluster models. Well developed quantum chemistry computer codes for clusters and molecules are available that have been optimized for their task. Alternatively, one may resort to supercell calculations, employing one of the codes designed for periodic boundary conditions. Thus, for solving practical problems, one may question the virtue of embedding schemes based on orbital space partitioning.

In this discussion, one has to keep in mind that the degree of approximation introduced by the fundamental embedding assumption strongly depends on the amount of virtual orbital admixtures. Hence, host crystals with a large band gap will be much less affected than semiconductors or even metals, and metals with a low density of states near the Fermi level will be less sensitive to the orbital space partitioning than metals like aluminum. Of course, the influence

of the embedding assumption also depends on the basis sets employed. Flexible, high quality basis sets with rather diffuse polarization functions will be more prone to these contaminations than rigid near-to-minimal basis sets. This observation also rationalizes the apparent success of test implementations of orbital basis partitioning schemes in the framework of semiempirical or tight-binding formalisms.^{36,38} Finally, the underlying electronic structure methods have to be considered, too. Wave function based Hartree–Fock derived methods are known to provide larger energy gaps and less polarizable states than density functional based methods.⁶⁵ In this respect, the present density functional investigation of defects in Li host clusters has to be regarded as a “worst case” study, and orbital space partitioning may perform better for other materials, basis sets, and electronic structure methods. Nevertheless, the present study clearly demonstrates the pitfalls associated with and the limitations of embedding schemes that are based on orbital space partitioning applied in a nonvariational fashion to density matrices within common SCF procedures.

ACKNOWLEDGMENTS

U.B. thanks C. Pisani for the many stimulating discussions. This work has been supported by the Deutsche Forschungsgemeinschaft via SFB 338 and by the Fonds der Chemischen Industrie.

- ¹J. A. Appelbaum and D. R. Hamann, *Phys. Rev. B* **6**, 2166 (1972).
- ²J. A. Appelbaum, G. A. Baraff, and D. R. Hamann, *Phys. Rev. B* **14**, 588 (1976).
- ³F. Máca and M. Scheffler, *Comput. Phys. Commun.* **51**, 381 (1988).
- ⁴J. E. Inglesfield, *J. Phys. C* **14**, 3795 (1981).
- ⁵G. A. Benesh and J. E. Inglesfield, *J. Phys. C* **17**, 1595 (1984).
- ⁶S. Crampin, J. B. A. N. van Hoof, M. Nekovee, and J. E. Inglesfield, *J. Phys. Condens. Matter* **3**, 1475 (1992).
- ⁷E. A. Colbourn, *Surf. Sci. Rep.* **15**, 281 (1992).
- ⁸K. M. Neyman and N. Rösch, *Chem. Phys.* **168**, 267 (1992).
- ⁹E. H. Teunissen, A. P. J. Jansen, A. B. van Santen, R. Orlando, and R. Dovesi, *J. Chem. Phys.* **101**, 5865 (1994).
- ¹⁰S. P. Greatbanks, P. Sherwood, and I. H. Hillier, *J. Phys. Chem.* **98**, 8134 (1994).
- ¹¹R. Bonaccorsi, R. Cimraglia, and J. Tomasi, *J. Comput. Chem.* **4**, 567 (1983).
- ¹²B. Wang and G. P. Ford, *J. Am. Chem. Soc.* **113**, 4776 (1991).
- ¹³T. Fox, N. Rösch, and R. J. Zauhar, *J. Comput. Chem.* **14**, 253 (1993).
- ¹⁴A. B. Kunz and D. L. Klein, *Phys. Rev. B* **17**, 4614 (1978).
- ¹⁵C. R. A. Catlow, M. Dixon, and W. C. Mackrodt, *Computer Simulation of Solids*, Springer Lecture Notes in Physics Vol. 166 (Springer, Berlin, 1982).
- ¹⁶A. B. Kunz, *Rev. Solid State Sci.* **5**, 181 (1991).
- ¹⁷A. R. Williams, P. J. Feibelman, and N. D. Lang, *Phys. Rev. B* **26**, 5433 (1982).
- ¹⁸P. J. Feibelman, *Phys. Rev. Lett.* **24**, 2627 (1985).
- ¹⁹P. J. Feibelman, *Phys. Rev. B* **35**, 2626 (1987).
- ²⁰P. Krüger and J. Pollmann, *Phys. Rev. B* **38**, 10578 (1988).
- ²¹P. Krüger and J. Pollmann, *Phys. Rev. B* **47**, 1898 (1993).
- ²²M. Scheffler, C. Droste, A. Fleszar, F. Máca, G. Wachutka, and G. Barzel, *Physica B* **172**, 143 (1991).
- ²³G. Wachutka, A. Fleszar, F. Máca, and M. Scheffler, *J. Phys. C* **4**, 2831 (1992).
- ²⁴A. J. Fisher, *Theor. Chim. Acta* **72**, 319 (1987).
- ²⁵C. W. Bauschlicher and P. S. Bagus, *Chem. Phys. Lett.* **90**, 355 (1982).
- ²⁶S. P. Walch, *Surf. Sci.* **143**, 188 (1984).
- ²⁷P. S. Bagus, C. W. Bauschlicher, C. J. Nelin, B. C. Laskowski, and M. Seel, *J. Chem. Phys.* **81**, 3594 (1984); **83**, 914 (1985).
- ²⁸G. Pacchioni, J. Koutecký, and H.-O. Beckmann, *Surf. Sci.* **144**, 602 (1984).
- ²⁹L. G. M. Pettersson and T. Faxen, *Theor. Chim. Acta* **85**, 345 (1993).
- ³⁰R. McWeeny, *Rev. Mod. Phys.* **32**, 335 (1960).
- ³¹S. Huzinaga and A. A. Cantu, *J. Chem. Phys.* **55**, 5543 (1971).
- ³²M. Kleiner and R. McWeeny, *Chem. Phys. Lett.* **19**, 476 (1973).
- ³³J. L. Whitten and T. A. Pakkanen, *Phys. Rev. B* **21**, 4357 (1980).
- ³⁴J. L. Whitten, *Phys. Rev. B* **24**, 1810 (1981).
- ³⁵J. L. Whitten, *Chem. Phys.* **177**, 387 (1993).
- ³⁶C. Pisani, *Phys. Rev. B* **17**, 3143 (1978).
- ³⁷C. Pisani, R. Dovesi, and P. Carosso, *Phys. Rev. B* **20**, 5345 (1979).
- ³⁸C. Pisani, R. Dovesi, and P. Ugliengo, *Phys. Status Solidi (b)* **116**, 249 (1983).
- ³⁹C. Pisani, R. Nada, and L. Kantorovich, *J. Chem. Phys.* **92**, 7448 (1990).
- ⁴⁰C. Pisani, F. Corà, R. Nada, and R. Orlando, *Comput. Phys. Commun.* **82**, 139ff (1994).
- ⁴¹C. Pisani and U. Birkenheuer, *Comput. Phys. Commun.* **96**, 152 (1996).
- ⁴²W. Ravenek and F. M. M. Geurts, *J. Chem. Phys.* **84**, 1613 (1986).
- ⁴³Y. Fukunishi and H. Nakatsuji, *J. Chem. Phys.* **97**, 6535 (1992).
- ⁴⁴S. Krüger and N. Rösch, *Chem. Phys. Lett.* **216**, 435 (1993).
- ⁴⁵S. Krüger, U. Birkenheuer, and N. Rösch, *J. Electron Spectrosc. Relat. Phenom.* **69**, 31 (1994).
- ⁴⁶S. Krüger and N. Rösch, *J. Phys. C* **6**, 8149 (1994).
- ⁴⁷B. Kirtman and C. de Melo, *J. Chem. Phys.* **75**, 4592 (1981).
- ⁴⁸C. E. Dysktra and B. Kirtman, *Annu. Rev. Phys. Chem.* **41**, 155 (1990).
- ⁴⁹K. A. Robins and B. Kirtman, *J. Chem. Phys.* **99**, 6777 (1993).
- ⁵⁰C. Pisani, *J. Mol. Catalyt.* **82**, 229 (1993).
- ⁵¹S. Casassa and C. Pisani, *Phys. Rev. B* **51**, 7805 (1995).
- ⁵²U. Birkenheuer, F. Corà, C. Pisani, I. Scorza, and G. Perego, *Surf. Sci.* (in press).
- ⁵³P. E. M. Siegbahn and U. Wahlgren, in *Metal-Surface Reaction Energetics*, edited by E. Shustorovich, (VCH, New York, 1991).
- ⁵⁴S. Priyadarshy, S. S. Skourtis, S. M. Risser, and D. N. Beratan, *J. Chem. Phys.* **104**, 9473 (1996).
- ⁵⁵U. Gutdeutsch, U. Birkenheuer, and N. Rösch (unpublished).
- ⁵⁶N. W. Ashcroft and N. D. Mermin, *Solid State Physics* (Saunders, Philadelphia, 1988), Table 4.2.
- ⁵⁷B. I. Dunlap and N. Rösch, *Adv. Quantum Chem.* **21**, 317 (1990).
- ⁵⁸S. H. Vosko, L. Wilk, and M. Nusair, *Can. J. Phys.* **58**, 1200 (1980).
- ⁵⁹N. Rösch, P. Knappe, P. Sandl, A. Görling, and B. I. Dunlap, in *The Challenge of d and f Electrons. Theory and Computation*, edited by D. R. Salahub and M. C. Zerner ACS Symposium Series Vol. 394 (ACS, Washington, DC, 1989).
- ⁶⁰C. Pisani and F. Corà, *Comput. Phys. Commun.* **82**, 179 (1994).
- ⁶¹F. Corà and C. Pisani, *Model. Simul. Mater. Sci. Eng.* **2**, 965 (1994).
- ⁶²P. Fantucci, V. Bonačić-Koutecký, and J. Koutecký, *Phys. Rev. B* **34**, 2777 (1986).
- ⁶³J. D. Head and S. J. Silva, *J. Chem. Phys.* **104**, 3244 (1996).
- ⁶⁴W. H. Fink, A. M. Butkus, and J. P. Lopez, *Int. J. Quantum Chem. Symp.* **13**, 331 (1979).
- ⁶⁵G. Pacchioni, K. M. Neyman, and N. Rösch, *J. Electron. Spectrosc. Relat. Phenom.* **69**, 13 (1994).